Microstructure analysis of “iron spots” on Qinghua porcelain from Jingdezhen imperial kiln

Wenxuan Wang, Philippe Sciau, Jian Zhu, Jianxin Jiang, Rui Wen, Magali Brunet

Microstructure analysis of "iron spots" on Qinghua porcelain from Jingdezhen imperial kiln

Wenxuan Wang [a], Philippe Sciau [b], Jian Zhu [c], Jianxin Jiang [d], Rui Wen [a], Magali Brunet [b]

[a] *China-Central Asia "the Belt and Road" Joint Laboratory on Human and Environment Research, Key Laboratory of Cultural Heritage Research and Conservation, School of Culture Heritage, Northwest University, 1 Xuefu Road, 710127 Xi'an, China*

[b] *CEMES-CNRS, 29 rue Jeanne Marvig, 31055 Toulouse, France*

[c] *Department for the History of Science and Scientific Archaeology, University of Science and Technology of China, 1129 Huizhou Road, 230026 Hefei, China*

[d] *Jingdezhen Institute of Ceramic Archaeology, 333001 Jingdezhen, China*

Abstract

"Iron spots" as a characteristic of early Qinghua porcelain is closely related to cobalt pigment and manufacturing technology. However, the microstructure of "iron spots" has not been fully investigated. Seventeen Qinghua samples with "iron spot" excavated in Jingdezhen imperial kiln were observed under stereomicroscope and SEM. Then, four representative sherds were systematically analyzed using FIB-TEM-EDX. Some ferrite solid solutions ($CoFe_2O_4$-Fe_3O_4 and Mn_3O_4-$MnFe_2O_4$-Fe_3O_4) are identified. $CaFeAlSiO_6$ and $Na_2Al_2Si_2O_6$-$CaAl_2Si_2O_6$ continuous solid solutions, as the main crystallites of "iron spot" are first reported. Moreover, we proposed that the dramatic increase of Fe or Mn in "iron spot" is caused by the source or formular change of cobalt pigment. Varieties of morphologies and species of the "iron spots" in Hongwu and Xuande reign implies that technology is under a transition period for adapting new formula, which provide a new perspective to discuss the use of cobalt pigments and technology development of Qinghua porcelain.

1. Introduction

Qinghua porcelain is one of the most influential cultural heritages of Chinese civilization in the world. Considering the heavy cobalt import dependence and the porcelain export demand in the 14^{th}-15^{th} century, the "raw material-production-consumption" cross-regional manufacturing and sales mode of Qinghua porcelain presented a predecessor of the global industrial chain division system [1–5].

Since the 1950s, aiming to identify the source of cobalt pigment of Qinghua porcelain, a set of cobalt source identification systems has been established based on the element ratios of Fe, Mn and Co, which is still widely used today [6–16]. And a consensus is generally accepted that a Fe-rich cobalt imported from Persia was used in imperial kiln until the Xuande reign (1426–1435 CE), a transition period when the domestic cobalt ore with a characteristic of high-Mn was begun to use. However, some scholars have raised doubts about this identification system based on chemical compositions. They suggested that the chemical compositions are insufficient to represent the original component information of the raw cobalt ore due to the influence of glaze matrix [17,18] and element differentiation in the treatment of cobalt pigment and the firing process [19–22].

On the contrary, from the perspective of ancient ceramics authentication and typology of traditional ceramic archaeology, the imported cobalt ore should be still used in Xuande reign (1426–1435 CE) of the Ming dynasty. Besides the similarity of the shape, decoration and blue-hue of Qinghua porcelain in Yongle (1403–1424 CE) and Xuande reign (1426–1435 CE), "iron spots" is considered as one of the criteria for the use of imported cobalt ores abundantly appearing only in the high concentration area of cobalt pigment on Qinghua porcelain in the early Ming Dynasty, especially in Yongle and Xuande reign [23]. It is of various forms with irregular convex or concave specks and different macro-views, also known as "black spot", "brown spot", "tin light" with different metallic luster [24]. Moreover, as a flaw, "iron spot" is caused by the immaturity of impurity removal, grinding, and firing processes in the early Ming dynasty. After the Xuande reign, "iron spots" gradually decreased, indicating the improvement of the manufacturing technology of Qinghua porcelain [23]. Thus, studying changes of "iron spots" from different periods provide a new angle not only to further understand the change of pigment source and recipe but also to explore the technology development of Qinghua porcelain.

Although "iron spots" in many researches were proved to contain dendrites or flower-like Fe-rich crystallites [25–28] of magnetite (Fe_3O_4) and cobalt ferrite ($CoFe_2O_4$) or Mn-rich crystallites [25,26, 29–30] of hausmannite (Mn_3O_4), jacobsite ($MnFe_2O_4$) and hausmannite-jacobsite intermediate compounds, the diversity and complexity of crystal species was not fully considered due to the small number of samples in previous studies, which is insufficient to fully reveal the microstructure of "iron spots" and chromogenic mechanism of different metallic luster. Furthermore, samples from one specific period also made it difficult to explain the above-mentioned cobalt source contradiction between traditional ceramic archaeology and scientific analysis, to discuss the connections and differences of the "iron spots" in different periods and summarize the characteristics of different technological development stages of Qinghua porcelain.

For accurately assessing the microstructure of "iron spots" on Qinghua porcelain without the influence of glaze matrix and element differentiation. Focused ion beam transmission electron microscopy coupled with energy-dispersive X-ray spectroscopy (FIB-TEM-EDX) was introduced in this study. It is an advantageous microstructure analysis method for studying ancient ceramics and has been successfully applied to illustrate the relationship between microstructure and porcelain manufacturing technology [31–34]. For Qinghua porcelain, Jiang [35] characterized the residual cobalt particles of Qinghua porcelain and proposed that the imperial kilns in the Xuande reign had begun to artificially mix domestic asbolane and imported smaltite to obtain cobalt blue.

In order to systematically identify the microstructure of "iron spots", firstly, 17 samples with "iron spots" selected from 72 sherds produced by the Jingdezhen imperial kiln in the Yuan dynasty (1271–1368 CE) and the Ming dynasty (1368–1644 CE) were observed and classified based on the micromorphology of "iron spots" by stereomicroscope and SEM. Then, the representative sherds were tested by FIB-TEM-EDX for further analysis of the submicron composition and crystallization microstructure. By exploring the relationship between the macroscopic appearance and microstructure of the "iron spots", the chromogenic mechanism of different metallic luster on "iron spots" is discussed, which provides a scientific basis for the authentication of Qinghua porcelain produced by the imperial kiln. The contradiction between

the identification characteristics and scientific analysis of "iron spots" in the Xuande reign of the Ming dynasty is also explained. Furthermore, by comparing and summarizing the characteristics of "iron spots" from different periods, the refined stages of Qinghua porcelain in the imperial kiln and enhanced the understanding of the cobalt source and technology evolution of Qinghua porcelain driven by historical and cultural internal causes from the 14th to 15th centuries.

2. Materials and methods

2.1. Samples description and preparation

All the studied samples have been excavated from the imperial kiln at Zhushan, Jingdezhen and were provided by the Jingdezhen Institute of Ceramic Archaeology. The Qinghua porcelain produced in imperial kiln were selected as research objects not only because the imperial kiln represents the highest level of craftsmanship in Qinghua porcelain making, but because the imperial kiln has stable supply of cobalt pigment and the strictest manufacturing processes, which made the "iron spots" presents stable change in micromorphology and microstructure from period to period. In contrast, "iron spots" almost ran through all the development stages of Qinghua porcelain made by folk kilns due to the unstable source of cobalt pigment (the impact of the war on international trade, the imperial kiln's control of high-quality imported cobalt resources and the expansion of market demand prompted folk kilns to use domestic cobalt ores since the Hongwu reign of Ming Dynasty) and the relatively simplified removal and firing process so that the change of "iron spots" caused by the improvement of technology can hardly be seen [36].

The samples from the Yuan Dynasty, Hongwu, and Chenghua can be distinguished according to their stratigraphic relationship. However, it is difficult for the samples from the Yongle and Xuan reign due to the proximity of their period and color. For distinguishing the samples from the Yongle and Xuan period, the sherds that can be jointed to the fragments with the Xuande reign mark and the sherds with the unique shape of the Xuande period such as cricket jar were selected. 1 sherd (Y-4) can be dated to the Yuan dynasty (1271–1368 CE) and 16 sherds can be dated to the Ming dynasty (1368–1644 CE) including 3 sherds (HW-2, HW-4, HW-5) from Hongwu reign (1368–1398 CE), 5 sherds (YL-2, YL- 6, YL-7, YL-9, YL-11) from Yongle (1403–1424 CE), 7 sherds (XD-1, XD- 2, XD-3, XD-4, XD-5, XD-6, XD-9) from Xuande (1426–1435 CE) and 1 sherd (CH-8) from Chenghua reign (1465–1487 CE). Figures of 17 samples are presented in Appendice (Fig. A1). The sherds with "iron spots" were mounted in epoxy resin and polished to obtain the morphological characteristics and microstructure of "iron spots" on Qinghua porcelain by SEM and FIB-TEM-EDX.

2.2. Stereomicroscope

A Nikon SMZ1000 stereomicroscope and a Keyence VHX-600 digital microscope in the laboratory of the Institute of Ancient Vertebrates and Ancient Humanities, Chinese Academy of Sciences, were used to observe the morphological features of the "iron spots".

2.3. FIB/SEM dual-beam system

Extraction of a TEM foil in the "iron spots" of Qinghua porcelain was performed using a dual-beam SEM/FIB FEI Helios 600i. The first step consists of the deposition of a Pt rectangular

layer of approximately 15 × 1 × 1 µm3 by EBID and [36] preventing the sample from structural defects and ion implantation damage caused by ion sputtering. Then, FIB trenches were cut on both sides of the platinum stripe, leaving in between a relatively thick foil of 15 × 5 × 1 µm3. Finally, using a sharp (approximately 1 mm) needle by a micromanipulator, the thick foil was extracted and carefully placed onto a Cu TEM mesh grid and then thinned up to approximately 100 nm.

2.4. TEM-EDX

All TEM experiments were performed in the laboratory of CNRS-CEMES. High-resolution bright-field images and selected area electron diffraction patterns were observed by a JEOL JEM 2010 TEM operating at 200 kV (JEOL Ltd, Japan). EDX mapping and chemical analyses were obtained by energy-dispersive X-ray spectroscopy (EDX) using a Philips CM20-FEG TEM, working at 200 keV and equipped with a Microanalyser QUANTAX XFlash detector with a 30 mm^2 active area and an energy resolution of 127 eV.

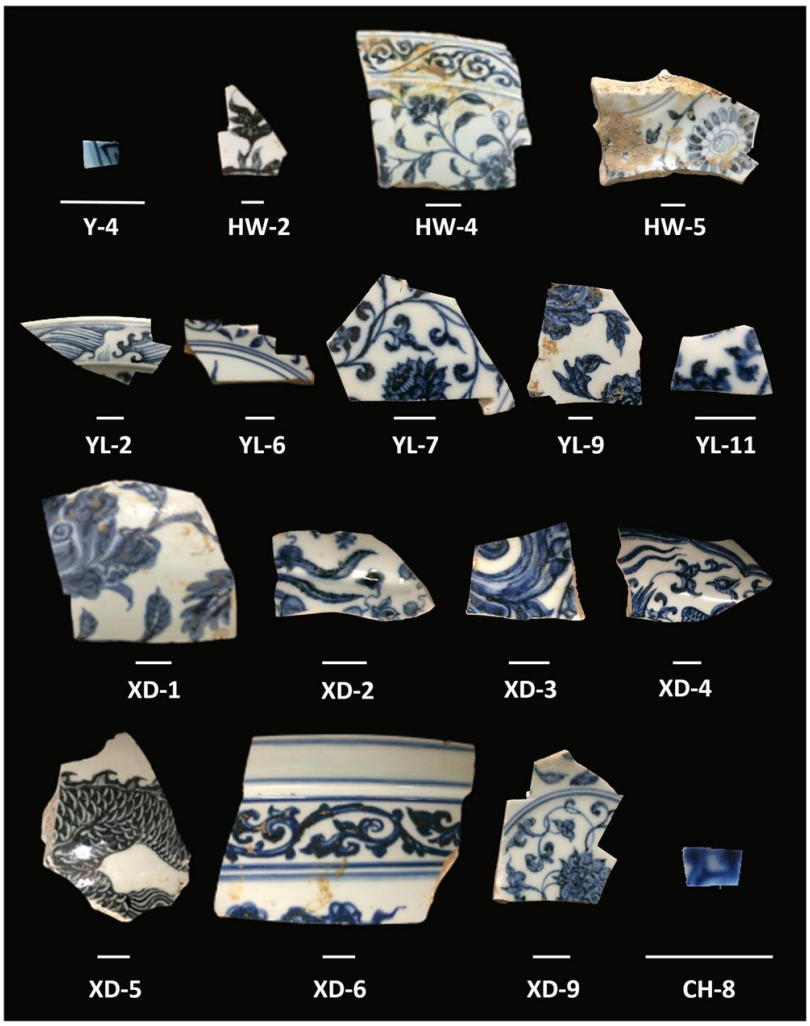

Fig. A1. The photograph of Qinghua porcelain sherds in imperial kiln from the Yuan dynasty (1271–1368 CE, refer to as Y) and Hongwu (1368–1398 CE, refer to as HW), Yongle (1403–1424 CE, refer to as YL), Xuande (1426–1435 CE, refer to as XD), Chenghua (1465–1487 CE, refer to as CH) reign of the Ming dynasty (1368–1644 CE) (scale bar: 2 cm).

3. Results

3.1. Micromorphology revealed by stereomicroscopy and SEM

17 sherds with "iron spots" were observed under the stereomicroscope and scanning electron microscopy to obtain the morphological characteristics of "iron spots" on Qinghua porcelain. Four typical micromorphological types of "iron spots" are summarized as following:

The first type is rare but shows obvious light points in HW-4 and XD- 1. SEM images show crystalline blocks with a length of 150 μm formed in the dense crystals area where octahedral crystals float on the glaze surface ranging from nanosized to 50 μm, which is inferred to be the main reason for the sparkling spots (Fig. 1a, e).

The second type shows a "tin light" with a metallic luster in part of samples such as HW-2, YL-6, XD-1, XD-2. Under a high magnification microscope, large dendritic crystals were observed. SEM images in backscattering mode show particularly developed, closely arranged, interlaced dendrites extending up to 100 μm. It can be found that the growth directions between primary and secondary dendrites and secondary and tertiary dendrites are perpendicular to each other, causing strong reflections of incident light. It is speculated that the large regular dendrites are the main cause of the "tin light" effect (Fig. 1b, f).

The third type is the most common one and presents in "iron spots" of all samples. This kind of spot is visually frosted grey and has no metallic luster from a macro perspective. SEM images show dendritic and hexagonal snowflake crystals with sizes varying from nanoscale to 30 μm. The heavy density of crystal nucleus made the room very limited to develop large dendrites with parallel branches. Therefore, it macroscopically shows visual grids with no glitter (Fig. 1c, g).

The last type of morphology shows brown specks in the samples of XD-1, XD-5 and XD-6. According to the shape of crystals in SEM images, they are massive reticular anorthite visible to naked eyes. In addition, phase separation structure can also be observed and is mostly concentrated in the gap between anorthite and its surroundings. Generally, the closer to the anorthite, the larger the phase-separation droplet size is, which illustrates that the phase separation structure was caused by precipitation of anorthite (Fig. 1d, h).

As mentioned above, "iron spots" present different macroscopic effects due to the different crystallization. Among them, the second and third type with dendrites and snow-like crystals have appeared in previous studies [26–30]. Yet the first and fourth type have never been reported. Generally, these different types of crystals do not occur alone but are often associated with each other, so it is insufficient to distinguish the different periods of Qinghua porcelain only by the occurrence of a single type of crystal. However, we found that specific crystallization patterns of "iron spots" might be used to generalize the Qinghua porcelain from the Yuan dynasty (1271–1368 CE) and the different periods of the Ming Dynasty (1368–1644 CE). The "iron spots" from the Yuan dynasty, and the Yongle (1403–1424 CE) and Chenghua reigns (1465–1487 CE) of the Ming dynasty show relatively stable crystallization composite patterns, where the second and third types of crystals are dendrites and snowflake crystals distributed around larger dendrites. In the Hongwu reign (1368–1398 CE), the patterns got more complicated. Except for the massive anorthite, all other remaining types of crystals are present. The most complex situation occurs in the "iron spots" from the Xuande reign (1426–1435 CE) with all the aforementioned types of crystals observed, which implies a change in the raw material and unstable firing technique.

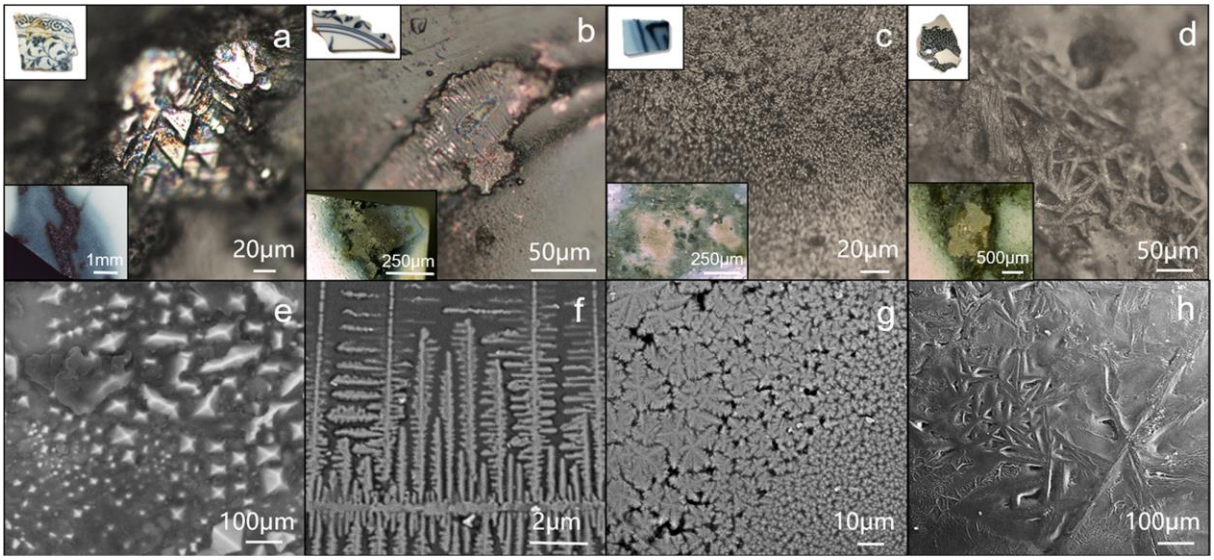

Fig. 1. (a-d) Stereomicroscope 3D digital images of 4 typical types of "iron spots" on the glaze surface with corresponding images of samples (upper left) and optical microscope images of "iron spots" (lower left); (e-h) SEM close-up images corresponding to a-d respectively.

3.2. Microstructure and chemical analysis by FIB-TEM

To explore the micromorphology, chemical compositions and microstructures of different "iron spots" on Qinghua porcelain, a dual system (FIB/SEM) in-situ foil (<150 nm) was extracted for TEM analysis.

In terms of the first type of spots, 1 sherd (HW-4) from the Hongwu reign (1368–1398 CE) was selected for foil preparation (Fig. 2a). The bright-field TEM image is shown in Fig. 2b-c. The crystalline block extends to approximately 3 μm under the glaze with column-like crystals grown underneath ranging from 100 nm to 500 nm. The crystal phases of the crystalline block and the column-like crystals analyzed by selected area electron diffraction (SAED) were identified as $CoFe_2O_4$ and $CaFeAlSiO_6$, respectively. Cobalt ferrite ($CoFe_2O_4$) belongs to the anti-spinel structure of the cubic crystal system. EDX mapping and selected area component testing were performed on the two distinct crystals. According to the element components of the selected areas (Table 1), the crystalline block should be a $CoFe_2O_4$-Fe_3O_4 solid solution doped with Mg, Al and a small amount of Mn ions (region 1). The downward column-like crystals are $CaFeAlSiO_6$ doped with Na, Mg and Co ions (region 2 and 3), which is identified to diopside. A well-developed diopside crystal is usually columnar consistent with the crystal morphology observed in the bright-field image. It is noted that the formation of $CaFeAlSiO_6$ is closely related to the crystallization of spinel. After the precipitation of spinel out of the molten glaze surface, calcium and aluminum was squeezed into the liquid phase around them. Then, diopside started to grow under the spinel and became the column-like crystals.

For the second and third types of dendrites and snow-flake crystals, we found spinel-structured crystals of 3 different compositions from different periods. Qinghua porcelain from the Yongle reign (1403–1424 CE) contains dendrites of $CoFe_2O_4$ in "iron spots", while Qinghua porcelain from both the Xuande (1426–1435 CE) and Chenghua reigns (1465–1487 CE) contains dendrites of $MnFe_2O_4$-Mn_3O_4 and $MnFe_2O_4$- Fe_3O_4 solid solutions, respectively.

A large dendrite with parallel branches of “iron spots” from the Yongle reign (1403–1424 CE) was selected as an example (YL-6) and then extracted for TEM foil preparation (Fig. 3a). Observing the bright-field image (Fig. 3b), the dendrites are approximately 0.2 μm in diameter with an intercolumn spacing of 0.5–1.2 μm. In addition, the undeveloped dendrites have quadrilateral cross-sections, whereas the developed dendrites grow at 90◦ along the four vertices of the quadrilateral, and all the secondary dendrites are perpendicular to each other, which shows the dendrite growth process. Liquid-liquid phase separation was also found as small droplets of approximately 10–150 nm in the amorphous glaze. The electron diffraction results prove that the dendrite is $CoFe_2O_4$. However, according to the selected area component testing (Table 1), the average atomic number of Fe/Co of dendrites in regions 1, 2 and 3 is 2.33, which is much smaller than that of the spinel-structured crystals from the Hongwu reign (the Fe/Co atomic number is 4.15). Thus, dendrites are more inclined to form a $CoFe_2O_4$-Fe_3O_4 solid solution with a small amount of Mg and Mn doping. Note that the compositions of dendrites slightly differ in regions 1, 2 and 3, suggesting a segregation phenomenon in the crystals that relates to a high degree of undercooling in the porcelain sintering process. Comparing the chemical components of phase-separated droplets (regions 4 and 5) and glaze (regions 6 and 7), Ca changed significantly. Considering the principle of crystallization and phase separation, the phase-separated droplets here were caused by the formation of cobalt ferrite crystals that led to a high- Ca environment.

As a representative for the Xuande reign (1426–1435 CE), XD-1 was selected to extract 2 TEM foil (L1 and L2) from the coexistence region of dendrite and phase separation in the glaze (Fig. 4a). The bright-field observation of L1 shows that dendrites are approximately 0.1–0.2 μm (Fig. 4b). The corresponding diffraction pattern along the [221] zone axis verifies a cubic anti-spinel structure similar to $CoFe_2O_4$ and it could be identified as ferromanganese crystals. These ferromanganese spinels could form at temperatures higher than 950 ◦C during the firing process of porcelain [37].

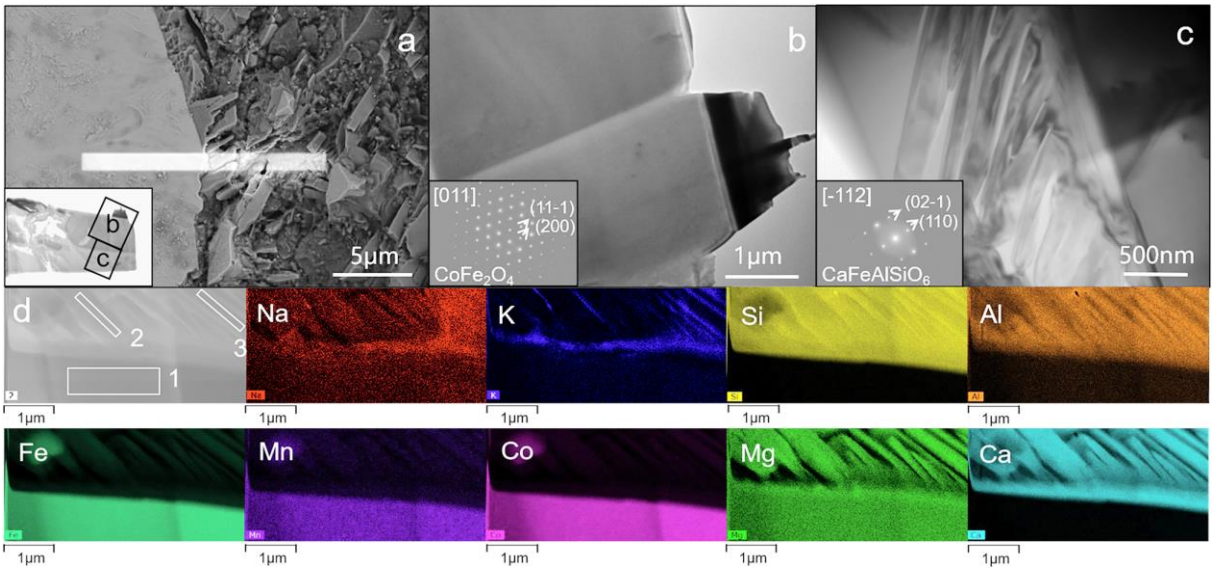

Fig. 2. (a) TEM preparation of HW-4 by FIB/SEM with deposition of the Pt protection (15 ×1μm2) and TEM foil after polishing (Lower Left); (b-c) Bright-field images of column-like crystals and crystalline block with corresponding electron diffraction pattern (Lower Left); A larger bright-field image (d) and the corresponding elemental maps of crystals of sample HW-4.

To accurately determine the chemical composition of the dendrites, a magnified bright-field (Fig. 4d) was selected to perform elemental distribution analyses (color images in Fig. 4) and selected area composition analyses. The results show that the dendrites are rich in Fe and Mn but absent of Si, Na, K and Ca, consistent with previous results. However, besides Fe and Mn, Co, Mg and Al are also significant in the crystals. According to the stoichiometric amounts of the elements (Table 1), the mean value of Fe/Mn ratios was calculated to be around 0.93, indicating an intermediate phase between the jacobsite ($MnFe_2O_4$) and hausmannite (Mn_3O_4): $MnFe_2O_4$-Mn_3O_4 solid solution. Besides, comparing the elemental composition of dendrites and glaze, partial substitutions of Co, Mg and Al could participate in forming a more complex compound (Mg^{2+}, Fe^{2+}, Mn^{2+}, Co^{2+}) (Fe^{3+}, Mn^{3+}, Al^{3+})$_2O_4$. The results confirm that the Mn amount in both crystals and glaze of the “iron spots” on fragments from the Xuande period is higher than that of fragments produced during the Hongwu and Yongle periods.

Table 1 Chemical composition of selected areas on samples (at%).

Sample	Selected area	Na	Mg	K	Ca	Mn	Fe	Co	Al	Si	O
HW-4	Crystal 1	0.04	3.23	0.08	0.09	0.91	35.48	8.55	1.46	0.27	49.89
	Crystal 2	0.99	4.65	0.29	12.56	0.14	6.04	0.93	5.16	20.91	48.34
	Crystal 3	0.36	4.47	0.08	12.53	0.13	5.65	0.85	4.98	20.86	50.10
YL-6	Crystal 1	0.12	1.47	0.16	0.36	0.69	28.26	12.47	3.18	3.61	49.68
	Crystal 2	0.31	1.77	0.20	0.23	0.73	28.40	11.99	3.22	2.53	50.62
	Crystal 3	0.25	1.33	0.25	0.50	0.65	27.04	11.42	3.42	4.32	50.81
	Droplet 4	0.21	0.13	1.06	4.61	0.05	0.74	0.18	6.81	25.64	60.57
	Droplet 5	1.49	0.17	1.79	5.50	0.06	0.60	0.31	6.92	24.33	58.81
	Glaze 6	0.72	0.08	1.19	2.58	0.04	0.72	0.30	7.42	27.84	59.12
	Glaze 7	0.97	0.06	1.66	2.89	0.02	0.68	0.26	7.65	27.82	57.99
XD-1 L1	Crystal 1	0.72	0.64	0.64	0.35	9.72	8.90	3.56	7.74	18.03	49.69
	Crystal 2	0.14	1.42	0.41	0.11	12.83	12.35	4.49	8.09	13.43	46.73
	Crystal 3	0.25	1.60	0.32	0.10	15.95	14.49	5.12	7.73	8.33	46.11
	Glaze 4	0.27	0.13	0.91	0.56	0.32	0.34	0.25	7.31	34.83	55.07
	Glaze 5	0.47	0.10	1.31	0.73	0.33	0.45	0.29	8.01	32.47	55.84
XD-1 L2	Crystal 1	3.24	0.10	0.32	4.74	0.18	1.24	0.27	14.16	26.08	49.68
	Crystal 2	3.29	0.03	0.46	4.46	0.27	1.54	0.22	14.43	26.22	49.08
	Crystal 3	3.21	0.09	0.32	5.05	0.26	1.01	0.27	13.68	25.42	50.70
	Droplet 4	0.60	0.96	0.83	1.09	9.14	10.04	2.69	3.96	20.52	50.19
	Droplet 5	0.13	1.38	0.40	0.61	13.40	11.41	2.90	2.25	16.89	50.61
	Droplet 6	0.82	1.20	0.48	0.95	10.60	8.12	2.57	4.44	22.62	48.22
CH-8	Crystal 1	0.54	0.64	1.35	0.26	6.94	23.33	9.18	7.49	2.40	47.86
	Crystal 2	0.41	0.78	0.35	0.22	6.00	22.96	8.83	7.16	0.50	52.79
	Crystal 3	0.24	0.78	0.26	0.14	6.05	23.73	9.33	6.71	0.67	52.10
	Glaze 4	0.58	0.15	1.84	0.86	0.29	0.38	0.24	7.29	26.72	61.66
	Glaze 5	0.89	0.16	2.40	1.06	0.35	0.40	0.25	8.01	27.06	59.43

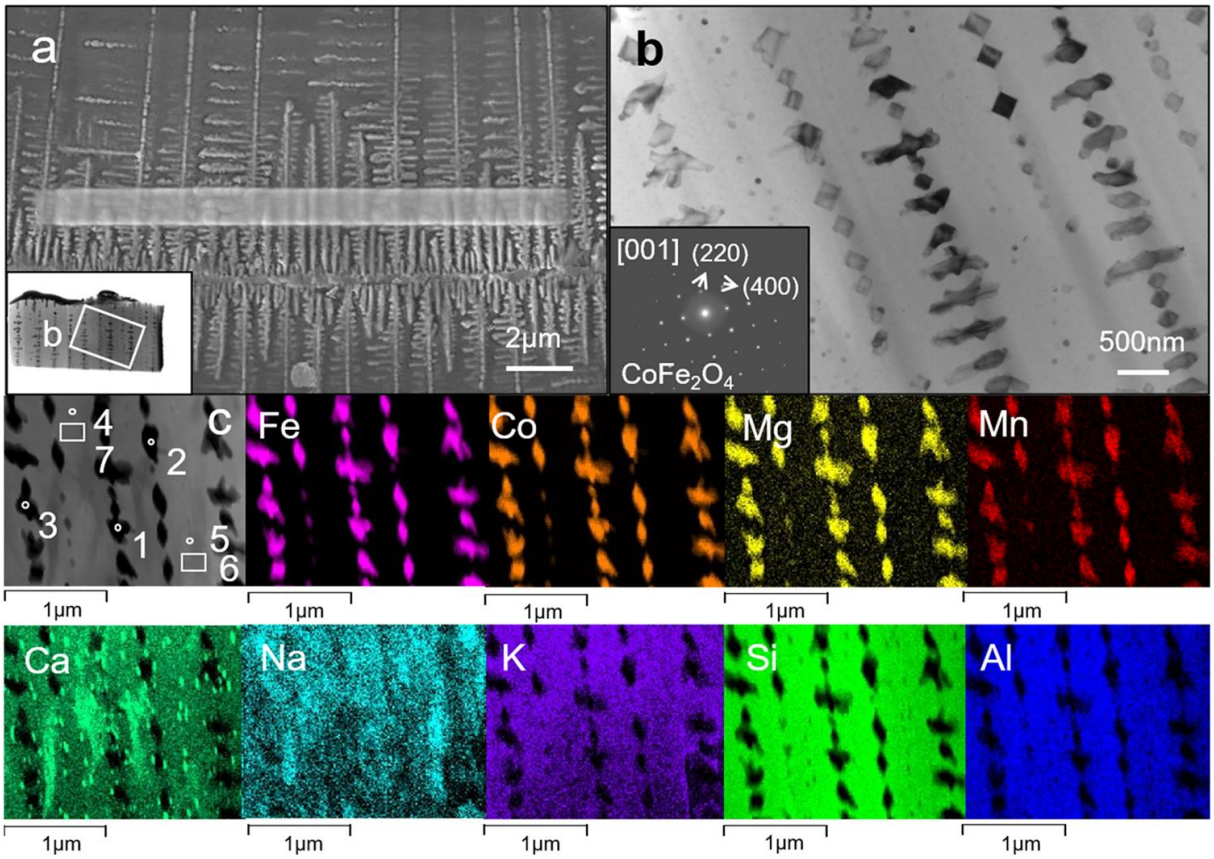

Fig. 3. (a) TEM preparation of YL-6 by FIB/SEM with deposition of Pt protection (15 ×1 μm2) and TEM foil after polishing (lower left); (b) bright-field images of dendrites with the corresponding electron diffraction pattern (lower left); A larger bright-field image (c) and the corresponding elemental maps of dendrites of sample YL-6.

The testing results of sample CH-8 from the Chenghua reign (1465–1487 CE) are included in Fig. 5 and Table 1. The SAED pattern of the crystal shows the [011] zone axis of face-centered cubic. The crystal plane spacing shows that the dendrite is $MnFe_2O_4$. Comparing the composition of dendrites (regions 1, 2, 3) and glaze (regions 4, 5), the EDX mapping and selected area analysis reveal that dendrites are rich in Fe, Co, Mn, Al, with a minor amount of Mg. Since the Fe/Mn of each region of the dendrite is higher than 2, the crystal should be a $MnFe_2O_4$- Fe_3O_4 solid solution, and a complicated compound (Mg^{2+}, Fe^{2+}, Mn^{2+}, Co^{2+}) (Fe^{3+}, Mn^{3+}, Al^{3+})$_2O_4$ can be identified.

The last type of crystal is present in XD-1 as well. The darker part in the middle of the bright-field image is anorthite surrounded by phase-separated droplets with sizes ranging from 10 nm to 400 nm (Fig. 4c). Mapping and selected area composition analysis were carried out in the area of anorthite and phase separation respectively. In addition to Ca, Al, and Si, anorthite (regions 1, 2, and 3) is also rich in Na (Fig. 6). Considering that Na+ and Ca+ in anorthite can be equivalently substituted to form a continuous solid solution, the column-like crystal here should be a $Na_2Al_2Si_2O_6$-$CaAl_2Si_2O_6$ continuous solid solution. The droplets in regions 4, 5 and 6 mainly contain Fe, Mn, Co and Mg, and they are speculated to be the phase separation structures caused by precipitation of the continuous solid solution (Table 1).

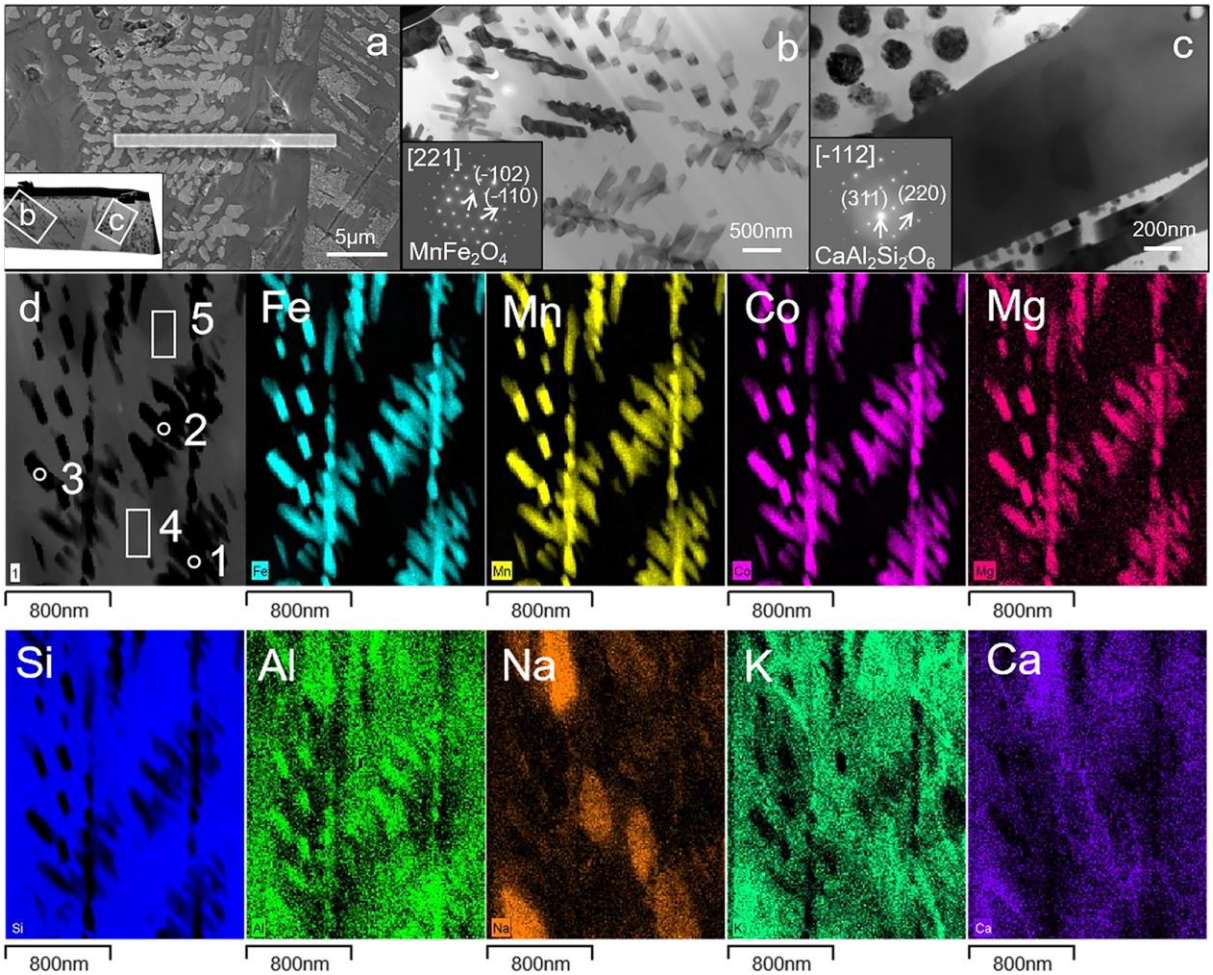

Fig. 4. (a) TEM preparation of XD-1 by FIB/SEM with deposition of Pt protection (15 ×1 μm2) and TEM foil after polishing (Lower Left); (b-c) Bright-field images of L1 and L2 respectively with the corresponding electron diffraction patterns (Lower Left); A larger bright-field image (d) and the corresponding elemental maps of dendrites of sample XD-1.

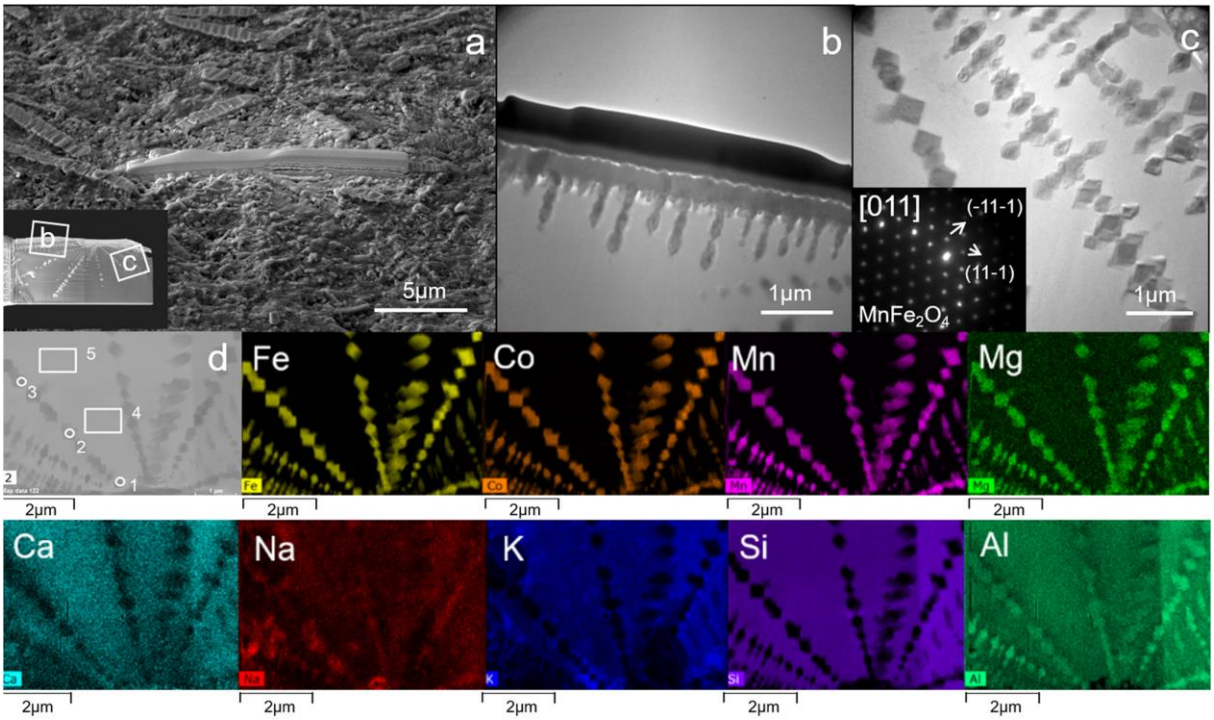

Fig. 5. (a) TEM preparation of CH-8 by FIB/SEM with deposition of Pt protection (15 ×1 μm2) and TEM foil after polishing (lower left); (b-c) Bright field images of dendrites with the corresponding electron diffraction pattern (upper left); A bright field image (d) and the corresponding elemental maps of dendrites of sample CH-8.

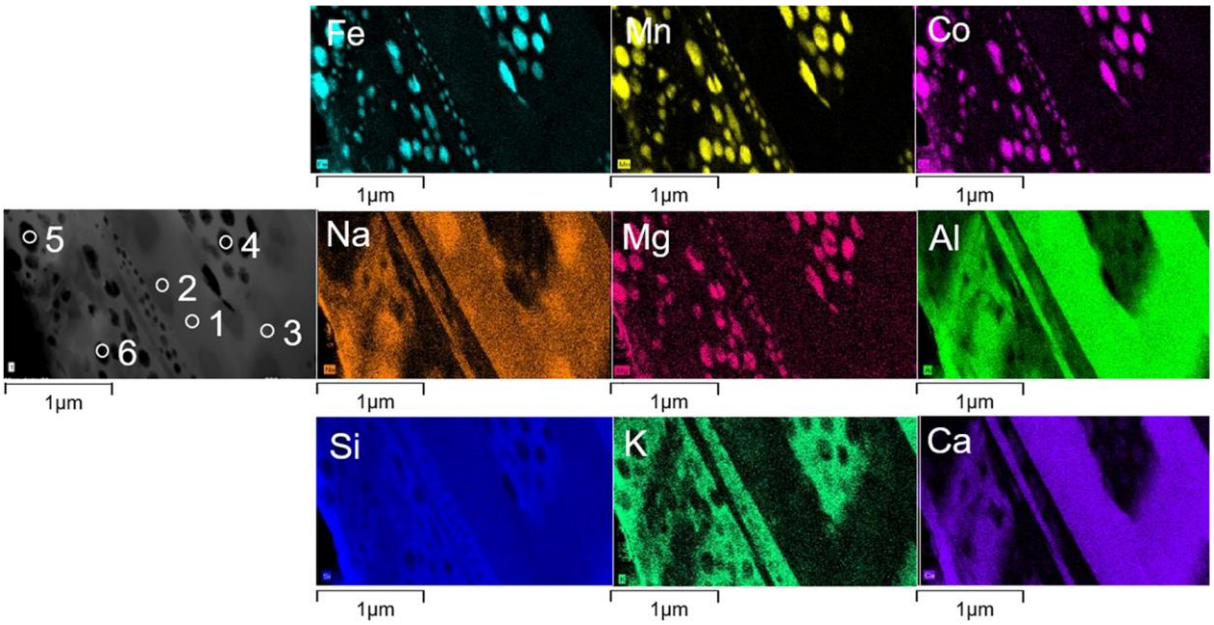

Fig. 6. A bright field image and the corresponding elemental maps of anorthite and phase separation droplets of TEM foil XD-2 L2.

4. Discussion

From a mainstream identification perspective, the presence of “iron spots” with metallic luster on Qinghua porcelain indicates the use of imported cobalt pigments with the characteristics of high-Fe and Low- Mn [23,24]. However, our findings indicate that “iron

spots" also occur on Qinghua porcelain that uses rich-Mn cobalt ore (domestic cobalt ore) in the Xuande and Chenghua reigns [11,35,38]. Thus, it is not reliable to distinguish the cobalt source of Qinghua porcelain according to the presence of an "iron spot". The main cause of this misunderstanding is that the most common crystals corresponding to different cobalt sources have a similar structure. Both the Co_3O_4-$CoFe_2O_4$-Fe_3O_4 solid solution related to imported cobalt ores and the Mn_3O_4-$MnFe_2O_4$-Fe_3O_4 solid solution related to local cobalt ores belong to the anti-spinel structure of the cubic system. As long as conditions are appropriate, "iron spot" in similar octahedral and dendritic form will generate on Qinghua porcelain whatever the imported cobalt ore with characteristics of high-Fe and low-Mn or domestic cobalt ore with characteristics of high-Mn and low-Fe is used. This is why some Qinghua porcelains with "iron spot" of the Xuande reign are mistaken for using the imported cobalt ore.

On the basis of microscopic morphology, chemical compositions and microstructures of the "iron spots" in different periods, we can further discuss the chromogenic mechanism of metallic luster, "iron spots" formation mechanism, the change of cobalt pigment recipe and technological development of Qinghua porcelain made by the imperial kiln. As a representative phenomenon on Qinghua porcelain in the 14th and early 15th century, "iron spots" have different macroscopic occurrences caused by different crystallizations. According to the microscopic morphology, a macroscopic point-flash of spot on Qinghua porcelain in Hongwu and Xuande reign is caused by regular octahedral crystals protruding from the glaze surface. As shown in SEM cross-section images in crystallization area of HW-4, the spinel-structured blocks only precipitated on the branch towards the glaze surface side and dendrites grow to the inner side of the glaze (Fig. A2).

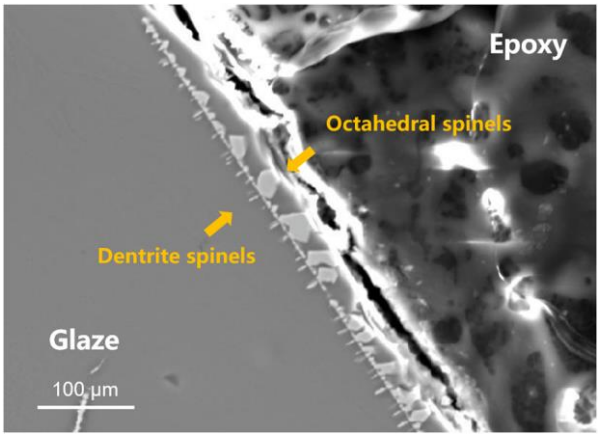

Fig. A2. SEM images of cross-section in spinel crystallization area of HW-4.

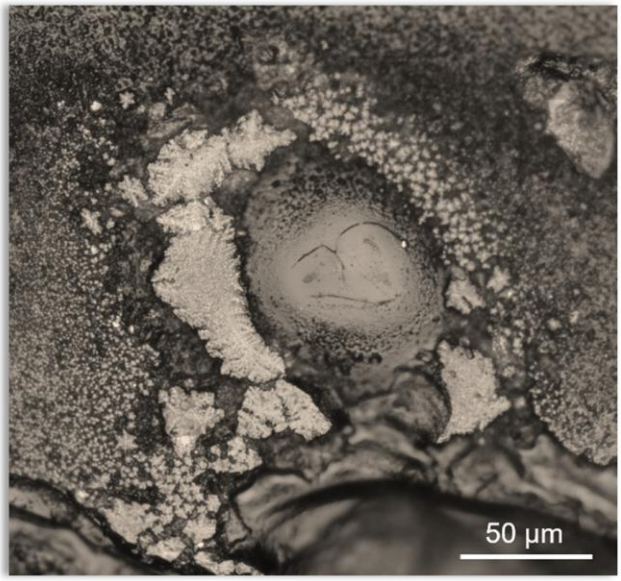

Fig. A3. Stereomicroscope 3D digital images of crystals around a bubble.

The developed dendrites with directional parallel branches tend to form the “tin light” spots. It is quite similar to the Fe2O3 crystals of “oil spot” in the Jian ware and brown glaze in Yaozhou kiln in which crystals are organized in a 2D periodic fashion [31,39]. Frosted spots (black, brown, and gray foggy spots without glitter) are mainly caused by dense dendritic and snowflake crystals from the nano to micron-scale with irregular configurations. The massively developed anorthite presents yellow or brown rusty spots in the Yuan and early Ming dynasties.

Based on the results, the formation mechanism of “iron spots” is discussed here. “Iron spots” are only found within the areas of blue decoration and never beyond the range of it, which infers that cobalt-blue pigment, not glaze, provides the crystallizing agent to form crystals. Cobalt pigment in early time was ground inadequately and remained impurity particles. The residual particles containing rich Fe or Mn crystal nucleuses are an essential prerequisite to form “iron spots” and dramatically reduced the nucleation barrier for the precipitation of newly generated rich Fe or Mn crystals, which is also called heterogeneous nucleation [40]. Heterogeneous nucleation also occurs at the phase interface like bubbles and glaze surface. As the temperature increases, the gas generated by the organic matter in the body and the carbonate, sulfate in the glaze, the O2 generated by the decomposition of Fe2O3 are wrapped in the glaze to form bubbles [41]. When the viscosity of the glaze melt decreases, under the action of surface tension, small bubbles merge into large bubbles and rise to the glaze surface. The cobalt impurity nucleuses enriched around residual particles on the interface of body and glaze will be brought up to the glaze surface by the bubbles. In the cooling process, some of the bubbles broke out of the surface and the surrounding glaze could fill the bubbles to make glaze surface smooth and flat again. If the cooling is too fast, the solidified glaze fails to the restore smoothness of the glaze surface and leave a pit. The growth of crystals is also the main reason to block the restoration of the glaze. A number of unfilled pits surrounded by crystals can be observed in “iron spots” on the glaze surface, which confirms the above deduction (Fig. A3). It also explains the reason why “iron spots” always show on the surface of glaze, though the cobalt pigment is painted between the body and

glaze. According to Tammann crystallization theory, when the glaze melt is cooled, heat preservation phase is required to make the nucleuses grow up. The difference in holding temperature and holding time can control the size and shape of crystals. In general, with faster cooling rates, smaller crystals are obtained [26]. In this case, the formation of crystals of different size and composition is likely to require a slow cooling rate.

In terms of the cobalt source, it is difficult to identify the specific cobalt source from chemical composition. Because “iron spot” is the secondary crystallization of cobalt ore after fully melting at high temperature, little information about the raw ore retained, especially trace elements with indicative significance, such as As, Cu, Ni, which are not found in samples. But it should be noted that the change of cobalt ores is obviously based on chemical composition of “iron spot” shown in the box diagram of Fe/Mn and Fe/Co at the “iron spot” in each period show in Fig. 7. This dramatic change due to the increase of Fe and Mn cannot cause by purification of raw material or firing process which only decrease the content of impurities but not increase. Pure cobalt does not exist in nature, but cobalt is present as an essential constituent in about 66 minerals [42], and as a minor or trace constituent of several hundred more, particularly those containing nickel, iron and manganese [43]. When cobalt-containing ores are used for blue pigments, iron and manganese in minerals will have a great impact on the color of Qinghua porcelain [44]. Thus, as impurities, iron and manganese need to be removed. Ancient literature described the use of magnets to remove iron from cobalt ores [45]. In addition, the high content of Fe and Mn is not introduced by the glaze, considering that the Fe content in the glaze is less than 1% and the Mn content is less than 0.1% [11].

The uprush of Fe/Co mainly caused by high-Fe content in Hongwu reign may be related to the pigment mixing. On the one hand, it is generally considered that the rapid development of Qinghua porcelain in Jingdezhen is affected by the under-glaze porcelain of Jizhou kiln where iron-bearing mineral was widely used in under-glaze porcelain and black-glazed porcelain. There are also cases of using iron oxide for outlining in blue-and-white porcelain from the Yuan dynasty, which shows the using of mixture of cobalt and iron oxide pigment. On the other hand, the Hongwu reign, the beginning of the Ming dynasty, was still in a socially unstable context of regime change. To consolidate the regime, the “maritime prohibition” policy greatly restricted imports, and non-government trade was also strictly prohibited [46,47]. In the meantime, land trade routes were also cut, given that the Ming dynasty had not yet fully controlled northern China [48]. The disruption of imported cobalt ores due to political instability forced craftsmen to change the formula of cobalt pigment [36]. Considering the consistency and inheritance of craftsmanship in the Jingdezhen imperial kiln, we believe that the dramatic change of Fe should be caused by the recipe change of blue pigment rather than the purification of raw material or firing process, which would only reduce the content of impurities but not increase the Fe/Co ratio. Due to the shortage of imported cobalt ore, it was possible to mix imported cobalt ore with iron-bearing mineral, resulting in the characteristics of black blue and “iron spot” with high-Fe in the Hongwu period. To adapt to the new formula, the purification and impurity removal and firing process need to be adjusted, so the “iron spots” on Qinghua porcelain in this period show complex crystallization composite patterns with high-iron.

After the brief social turmoil from the late Yuan to the early Ming dynasty and the 30-year economic recovery in the Hongwu reign, the political situation was stable in the Yongle reign.

The government established friendly diplomatic relations and trade with overseas countries and started the famous Ming treasure voyages (Zheng He's voyages) [49]. During this period, imported cobalt materials were reliable and the "iron spots" also showed similar crystallization with stable morphology and composition. The sharp drop of Fe/Mn mainly caused by the increase of Mn in Xuande and Chenghua reign indicates the domestic cobalt ore with high- Mn used in this period. During the Xuande reign, with the further expansion of both the internal and external demand, expensive imported cobalt ores were difficult to meet the large demand for Qinghua porcelains, but the Ming government stopped Zheng He's navigation activities and implemented the "maritime prohibition" policy again [50, 51]. As a consequence, the imperial kiln began to explore domestic cobalt ores as an alternative to the imported cobalt pigments.

The sharp drop in Fe/Mn mainly in the Xuande and Chenghua reigns caused by the increase in Mn indicates the use of high-Mn domestic cobalt ore or a mixed pigment of imported and domestic cobalt ore in this period, which is consistent with previous studies [11,35,38]. In the process of adapting to new materials, the "iron spots" in this period show a variety of morphologies and complex compositional characteristics with Mn-based spinel structures and well-developed anorthite. After improved manufacturing technology and stable source of domestic cobalt ores, Qinghua porcelain in the Chenghua reign had a stable color, and the "iron spots" showed a relatively single crystallization composite pattern with manganese ferrite but then gradually vanished.

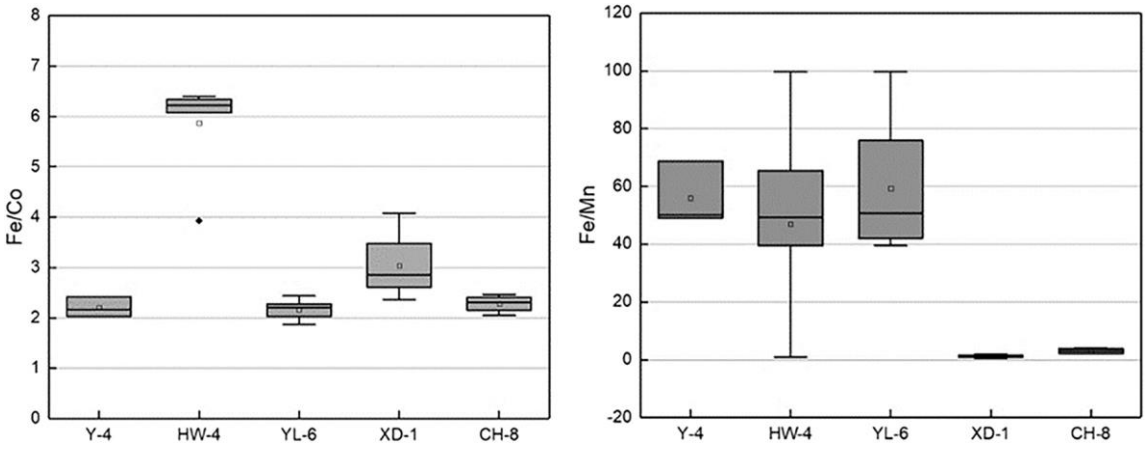

Fig. 7. Box plot of Fe/Mn and Fe/Mn ratio of "iron spot" on Qinghua porcelain of 5 samples.

5. Conclusion

This study reveals the micro-morphology, chemical composition and microstructure of "iron spot" on the Qinghua porcelain manufactured by imperial kiln in Jingdezhen in 14th-15th century. Besides $CoFe_2O_4$- Fe_3O_4 and Mn_3O_4-$MnFe_2O_4$-Fe_3O_4 solid solutions, $CaFeAlSiO_6$ and $Na_2Al_2Si_2O_6$-$CaAl_2Si_2O_6$ continuous solid solution as the main crystallization of "iron spots" are found for the first time. The contradiction related to "iron spot" is explained: "iron spot" is definitely not a symbol of imported cobalt ores, because whether imported or local cobalt ores are both capable of forming "iron spots" of different ferrite spinel solid solutions but with same anti-spinel structure. Then, the relationship between macro-morphology and

microstructure is revealed: the point-flashed spot and “tin light” spot is caused by spinels and developed dendrites with directional parallel branches respectively. The formation mechanism is also clarified. Furthermore, crystallization composite patterns of “iron spots” in different periods have unique characteristics. The dramatic increase of impurity elements like Fe and Mn was caused by the source or recipe change of cobalt pigment. The diversity of “iron spots” crystal morphology and species in a certain period was related to the exploration stage caused by adapting new raw materials. It is also pointed out how pigment formula and the technology of Qinghua porcelain changed and developed under the influence of foreign trade policy from 14^{th} to 15^{th} century.

Declaration of Competing Interest

The authors declare that they have no known competing financial interests or personal relationships that could have appeared to influence the work reported in this paper.

Acknowledgments

Thanks to the Jingdezhen Ceramic Archaeological Institute for providing samples, and especially Shurong Wu for sample selection. We also thank Cécile Marcelot and Sébastien Joulié for their technical assistance with the experimental work; Yuanqiu Li and Tian Wang for their aid in data analysis. This study was sponsored by the China Postdoctoral Science Foundation Project (2020M67361) and the Shaanxi Provincial Department of Education Key Laboratory Research Project 20JS147).

References

[1] J. Rawson, The lotus and the dragon: sources of Chinese ornament, Orientat 15 (1984) 22–36.

[2] J.Z. Li, History of Science and Technology in China, Ceramics Volume, Science Press, Beijing, 1998.

[3] M. Cowell, F. Zhang, Analyses and source of the cobalt blue pigment employed on Chinese ceramics, British Museum Press, London, 2001, pp. 601–605.

[4] N.W.R. Kerr, High-Firing Colours: Copper, iron and cobalt” in Science and Civilisation in China, vol. 5, Cambridge University Press, 2004.

[5] R. Giannini, I.C. Freestone, A.J. Shortland, European cobalt sources identified in the production of Chinese famille rose porcelain, J. Archaeol. Sci. 80 (2017) 27–36. [6] S. Young, An analysis of Chinese blue-and-white, Orient. Art. 2 (1956) 43–47.

[7] S.H.M. Garner, The use of imported and native cobalt in Chinese blue and white, Orient. Art. 2 (1956) 48–50.

[8] M.J.M. Banks, M S Furth., Anal. Chin. blue–White *Archaeom.*, 10, 1967, pp. 101–103. [9] W. J notes on the use of cobalt in later Chinese ceramics Ars Orientalis Orient. Art., 11, 1979, pp. 63–85.

[10] Y.C. Chen, An investigation on Chinese blue-and-white ware and its blue pigment, J. Chin. Ceram. Soc. 6 (1978) 225–241.

[11] R. Wen, C. Wang, Z. Mao, Y. Huang, A. Pollard, The chemical composition of blue pigment on Chinese blue-and-white porcelain of the Yuan and Ming dynasties (AD 1271–1644), Archaeometry 49 (2007) 101–115.

[12] Y.C. Chen, in: Qing Hui, H.J. Luo, X.M. Zheng (Eds.), Scientific explanation, Shanghai Science and Technical Literature Press, Shanghai, 2009, pp. 351–360.
[13] H. Li, et al., Origin characteristics and causes of cobalt dispersion on Qinghua Porcelain of Guan kiln in early ming dynasty, Sci. Conserv. Archaeol. 30 (2018) 30–36.
[14] M.A. Pollard, M. Matin, From ore to pigment: a description of the minerals and an experimental study of cobalt ore processing from the Kshn, Mine, Iran, *Archaeometry* (2017).
[15] N. Wood, M.S. Tite, C. Doherty, B. Gilmore, A technological examination of ninth-tenth century AD Abbasid blue-and-white ware from Iraq, and its comparison with eighth century AD Chinese blue-and-white sancai ware, Archaeom 49 (2010) 665–684.
[16] R. Wen, A.M. Pollard, The pigments applied to islamic minai wares and the correlation with Chinese blue-and-white porcelain, Archaeom 58 (2016) 1–16.
[17] Q. Ma, M. Pollard, J. Jiang, Y. Weng, An evaluation of quantitative XRF analysis applied to determine cobalt sources in Chinese blue and white porcelain, Archaeom 63 (2020) *194–203*.
[18] R. Zhang, P. Gethin, Provenance of the cobalt pigment used for Jingdezhen minyao blue-and-white porcelain in the early qing dynasty, Ceram. Int. 47 (2021) 25763–25768. [19] Y. Zhu, Tao Shuo (1774). [20] Z.M. Wang, Chorography of Jiangxi Province (Ceramics Volume, 1556).
[21] R. Wen, A. Pollard, Comparative study of cobalt blue pigment on Chinese blue-and-white porcelain and Islamic glazed pottery, thirteenth-seventeenth centuries, Sci. Res. Hist. Asian Ceram. (2009) 24–32.
[22] T. Zhu, X. Ding, C.M. Kusimba, Z. Feng, Using laser ablation inductively coupled plasma mass spectroscopy (LA-ICP-MS) to determine the provenance of the cobalt pigment of Qinghua porcelain from Jingdezhen in Yuan Dynasty of China (1271–1368AD), Ceram. Int. 41 (2015) 9878–9884.
[23] B.C. Geng, Identification of Porcelain in Ming and Qing Dynasties, Forbidden City Press, Beijing, 1993, p. 523.
[24] Y. Zhou, Q. Zhou, Trace Types and Evidence Identification of Qinghua in Yuan Dynasty, Nanfang Daily Press, Guangdong, 2014, p. 490.
[25] J. Wu, J. Li, Z.Q. Deng, C.S. Wang, Dating research on blue-and-white porcelain of Jingdezhen official kiln, Sci. China Ser. E: Eng. Mater. Sci. 34 (2004) 516–524.
[26] Wu J, P.L. Leung, Li J, A study of the composition of Chinese blue and white porcelain, Stud. Conserv. 52 (2007) 188–198.
[27] W. Wang, et al., Microscopic analysis of "iron spot" on blue-and-white porcelain from Jingdezhen imperial kiln in early Ming dynasty (14th-15th century), Microsc. Res. Tech. 79 (2016) 1123–1130.
[28] T. Wang, et al., Raman study of Yuan Qinghua porcelain: the highlighting of dendritic CoFe2O4 crystals in blue decorations, J. Raman Spectrosc. 48 (2017) 267–270.
[29] A. Pinto, P. Sciau, T. Zhu, B. Zhao, J. Groenen, Raman study of Ming porcelain dark spots: probing Mn-rich spinels, J. Raman Spectrosc. 50 (2019) 711–719.
[30] J. Roqu´e-Rosell, et al., Synchrotron XAS study of Mn and Fe in Chinese blue-and-white Ming porcelains from the second half of the 15th century, Ceram. Int. 47 (2021) 2715–2724.
[31] C. Dejoie, et al., Learning from the past: rare ε-Fe2O3 in the ancient black-glazed Jian (Tenmoku) wares, Sci. Rep. 4 (2014) 1–9.

[32] J. Hou, T. Pradell, Y. Li, J. Miao, Jun ware glazes: chemistry, nanostructure and optical properties, J. Eur. Ceram. Soc. 38 (2018) 4290–4302.
[33] Z. Liu, et al., The morphology and structure of crystals in Qing Dynasty purple-gold glaze excavated from the Forbidden City, J. Am. Ceram. Soc. 101 (2018) 5229–5240.
[34] J.A. Cui, et al., A short but glorious porcelain glaze of early ming dynasty: new finding of raw material and colorants in the copper red glaze, J. Eur. Ceram. Soc. 41 (2021) 3809–3815.
[35] X. Jiang, et al., Early globalized industrial chain revealed by residual submicron pigment particles in Chinese imperial blue-and-white porcelains, Proc. Natl. Acad. Sci. U.S.A. 117 (2020) 6446–6452.
[36] H. Cheng, B. Zhang, J. Wang et al., 2005. A PIXE study on the folk blue ang white porcelains made in Yuan, Ming and Qing Dynasties in Jingdezhen. Science and technology of Ancient Ceramics 6:Proceedings of International Symposium (ISAC'05), Shanghai Science and Technology Literature Press Shanghai 167 171.
[37] F. Schweizer, A. Rinuy, Manganese black as an Etruscan pigment, Stud. Conserv. 27 (1982) 118–123.
[38] Z. Bao, H. Yuan, R. Wen, K. Chen, The fast and direct characterization of blue-and-white porcelain glaze from Jingdezhen by laser ablation-inductively coupled plasma mass spectrometry, Anal. Methods 7 (2015) 5034–5040.
[39] Q. Hoo, X. Wang, Y. Sun, et al., Formation mechanism of the pinholes in brown glazed stoneware from Yaozhou kiln, Archaeom 64 (2022) 644–654.
[40] P.W. Lu, Fundamentals Inorganic Materials Science, Wuhan University of Technology Press,, Wuhan, 2009, pp. 264–266.
[41] T. Pradell, J. Molera, Ceramic technology How Character Ceram. glazes. *Archaeol. Anthr. Sci.,* 12, 2020, p. 189.
[42] B. Lafuente, R.T. Downs, H. Yang, N. Stone, The power of databases: The RRUFF project, De Gruyter (O), 2015, pp. 1–30.
[43] J.D. Donaldson, D. Beyersmann, Cobalt and cobalt compounds, Ullmann's Encycl. Ind. Chem. (2000).
[44] A. Pinto, J. Groenen, B. Zhao, T. Zhu, P. Sciau, Chromogenic mechanisms in blue-and-white porcelains, J. Eur. Ceram. Soc. 40 (2020) 6181–6187.
[45] Y. Zhu, Tao Shuo, 1774. [46] Y. Zhong, D. Qin, K. Li, Export and characteristics of Jingdezhen porcelain in middle ming dynasty, Cult. Relics 11 (2020) 49–66.
[47] A. Schottenhammer, Imperial maritime China. Oxford Research Encyclopedia of Asian History, Oxford University Press, 2019.
[48] Y. Hu, Foreign policies in Hongwu and Yongle periods of Ming Dynasty, J. Northwest Minzu Univ. Philos.: Soc. Sci. Ed. 3 (1987) 5.
[49] Ming Tai Zong Shi Lu (1430).
[50] J. Wei, The globalization of porcelain trade in the 16-17th century: centered on shipwreck data, J. Palace Mus. 2 (2022) 4–16.
[51] R.M. Brown Ming Ban-Ming Gap: Southeast Asian Shipwreck Evidence for Shortages of Chinese Trade Ceramics Hwa Chung Proceedings of the International Conference: Chinese Export Ceramics and Maritime Trade 2005 12th–15th Centuries Hong Kong 78 104.